Experimental study on dielectric barrier discharge actuators operating in pulse mode

M. Kotsonis[a] and L. Veldhuis
Faculty of Aerospace Engineering, Delft University of Technology, Kluyverweg 1, Delft 2629HS, The Netherlands

(Received 23 July 2010; accepted 20 October 2010; published online 9 December 2010)

An experimental investigation is performed on the operation of dielectric barrier discharge plasma actuators used as manipulators of secondary and unsteady flow structures such as boundary layer instabilities or shedding vortices. The actuators are tested mainly in pulse mode. High sample rate hot-wire measurements of the induced velocity field downstream of the actuator are taken for the cases of pulse actuation in still air as well as in a laminar boundary layer. Complementary voltage and current measurements are taken to calculate power consumption. Additionally, a study on the influence of the pulse frequency and duty cycle of actuation is performed. Results show the effectiveness of plasma actuators in inducing fluctuating components of velocity when operated in pulse mode. Spectral analysis reveals the connection between the actuator driving signal and the induced flowfield. The magnitude as well as the consistency of the resulting fluctuating field are dependent on both the duty cycle and the pulse frequency. An empirical operational envelope based on phenomenological observations is proposed, for the use of the actuators at specific flow and operational conditions given in the paper. © *2010 American Institute of Physics*.
[doi:10.1063/1.3517453]

I. INTRODUCTION

Plasma actuators have been in the interest of the flow control community for the last ten years.[1–5] Their simple construction, robustness, and low power requirements render them ideal for active flow control in a variety of scenarios. Numerous studies have been performed in utilizing these actuators, among others, for airfoil separation control[6,7] and boundary layer control.[8–10] Several parametric and optimization studies have been performed for maximizing the produced body force and induced velocity.[11–16] More recently the use of advanced techniques such as nanopulse discharges[17,18] and three-electrode designs[19] have been proposed. The general consensus of these studies is that although the actuators have the potential for efficient flow control at low velocity regimes, their effectiveness decreases with increased Reynolds number. This is based on the limited momentum input the actuator can provide to the flow. Limitations arise from several factors such as dielectric strength and thickness of the dielectric layer, breakdown voltage of air and geometric configuration of the actuator. Typical maximum induced velocities do not exceed the threshold of 10 m/s for the conventional dielectric barrier discharge (DBD) actuators. In order to efficiently control natural flows with such a small momentum input, one must turn to the secondary structures or instabilities of the global flow dynamics. One typical example of low power flow control is the delay of laminar-turbulent transition by means of Tollmien–Schlichting (TS) wave cancellation. This technique aims at tackling the instability waves while still at linear amplification stage. At this stage the waves have little energy content with typical amplitudes of 0.01% of the freestream velocity.[20] By controlling these instabilities at the initial low-energy stages, the evolution of the global hydrodynamic chain can be changed with minimum actuation energy. Similar technique has already been investigated with the use of vibrating membranes as actuators.[21] In recent studies[22,23] artificially introduced TS waves were successfully cancelled using plasma actuators. These structures are typically unsteady and as such require unsteady actuation for optimal control. Investigations on manipulating other unsteady structures such as shedding vortices using the actuator in pulse mode have been performed.[24,25]

Although the pulse mode has been verified to be equally or in some cases more effective than continuous operation,[18,24] plasma actuators under pulse operation and the resulting flowfield have yet to receive detailed investigation as a stand alone phenomenon. A limited number of studies[26–28] have been published on the subject. The aim of this paper is to further investigate the behavior of the plasma actuator and the response of the surrounding flow under pulse operation. More specifically, this will be done both for the case of still air as well as for the case of the actuator operating in a laminar boundary layer. Furthermore we aim at identifying the sensitivity and behavior of the induced flow, under the variation in the pulse frequency and duty cycle of actuation. This will provide an insight on the potential and limitations of these devices for applications that involve low power flow control based on manipulation of instabilities or other secondary flow structures.

II. EXPERIMENTAL SETUP

A. The actuator

For this study the conventional DBD actuators are used. The actuators consist of thin rectangular copper electrodes

[a]Electronic mail: m.kotsonis@tudelft.nl.

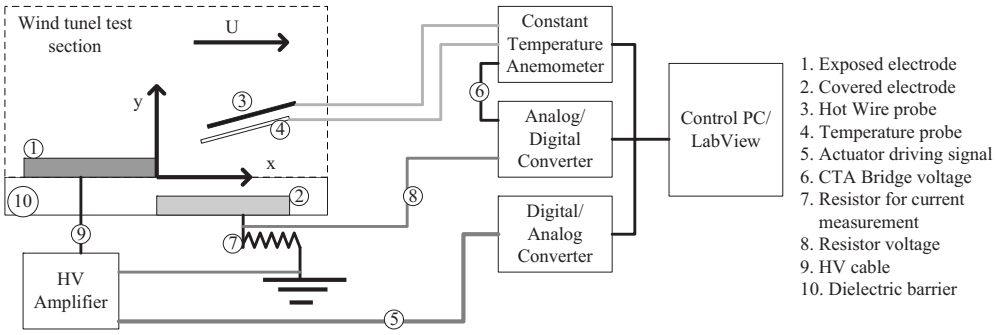

FIG. 1. The experimental setup and coordinate system (not to scale).

made out of self-adhesive copper tape separated by a dielectric layer (Fig. 1). The thickness of both electrodes is 60 μm and the width is 10 mm. Their effective spanwise length (along which plasma is generated) is 200 mm. The electrodes are separated by two Kapton tape layers. The thickness of each layer is 2 mil (50.8 μm). The total thickness of the dielectric (including adhesive) is approximately 110 μm.

The electrodes and dielectric are supported by a 10 mm thick, 200×100 mm^2 rectangular polyoxymethylene plate carrying two aluminum connectors. The connector of the upper electrode is connected to the high voltage (HV) output cable of a TREK 20/20C HV amplifier ($\pm$20 kV, $\pm$20 mA) while the connector of the lower electrode is grounded. The actuator operation is controlled remotely via a computer workstation were the driving signal is created by LABVIEW software and is sent to the amplifier via a digital/analog converter. The amplifier provides direct readings of the output voltage while the output current is measured using the voltage across a resistance (100 Ω) placed between the lower electrode and the grounding cable.

B. Measurements setup

The measurements are conducted in the test section of the boundary layer tunnel (BLT) at the TU Delft. This windtunnel is of the closed type with a test section of $1.5\times0.3\times5$ m^3. The tunnel incorporates a flexible wall which allows the creation of a large variety of pressure gradients. The boundary layer is formed on the opposite smooth plate. A knife edge protruding slightly into the flow ensures that the incoming turbulent boundary layer, formed in the contraction ratio, is bled out and a clean laminar boundary layer is initiated at the leading edge. The velocity range of the tunnel ranges from 1 to 40 m/s while freestream turbulence intensity is lower than 0.09%.

For the flow diagnostics the use of hot wire anemometry (HWA) is selected. HWA has been used in previous studies involving plasma actuators[10,29] and has been found best suited for a parametric study as it combines sufficient accuracy, high sampling rate and relative ease of use. For this study a constant temperature anemometer (TSI Inc. Model IFA300) is used with a single cylindrical hot film sensor model 1201-20. The sensor has been calibrated using a TSI 1127 calibrator configured for a range of velocities between 0 and 12 m/s. During the measurements, temperature readings in the proximity of the sensor are taken for velocity correction. Typical ΔT for a single measurement sequence is in the order of 0.5 °C for quiescent flow. No measurable difference has been found in the case of boundary layer flow. The hot-wire probe is traversed using a manual three-component traversing system with a 0.1 mm accuracy in each direction.

Based on an initial two-dimensionality study, the flow has been identified as uniform and constant along approximately 80% of the span of the electrodes. Some edge effects are present due to the assymetry near the ends of the actuator which have negligible influence to the center part flowfield. Based on this, any velocity component in the spanwise direction is considered negligible and the probe is placed in order to measure total velocity, U. Based on results from a previous particle image velocimetry (PIV) study,[30] the vertical velocity component v is considered negligible in the downstream region compared to the horizontal component u. Nevertheless, all measurements will be presented in the form of total velocity. All measurements are taken at the half-span of the actuator. For all distance references in this paper the coordinate system presented in Fig. 1 is used. The origin of the axes is located at the downstream edge of the exposed electrode. To sufficiently resolve the temporal evolution of the flow and increase the accuracy of the spectral analysis, a sampling rate of 50 kHz is chosen with varying sampling time, depending on the distance of the hot-wire probe from the actuator.

Three x positions are selected at 7, 12, and 17 mm downstream the actuator. At these positions measurements are taken at selected y positions near the wall. Additionally, for the case of the laminar boundary layer, two more downstream positions at 43 and 93 mm are measured in order to track any convecting structure that might be initiated from the operation of the actuator.

For the entire study the high-voltage signal is kept fixed at $V_{pp}=10$ kV with a carrier frequency (f_{ac}) of 2 kHz. The operation of the actuator in pulse mode is essential for the manipulation of unsteady flow structures. As such the actuation period can be separated into the "on" and "off" stage. The pulse frequency (f_p) is defined as the number of times the actuator switches on and off while the duty cycle (D) is the percentage of the time period the actuator is on over one full actuation period [Eq. (1)].

$$D=\frac{t_{on}}{t_{on}+t_{off}}100=t_{on}f_p100. \tag{1}$$

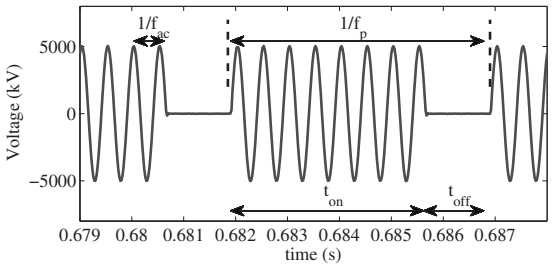

FIG. 2. Sample of the voltage signal with the characteristic actuation values. (f_p=200 Hz and D=75%).

A schematic of a typical actuation signal is shown in Fig. 2. To investigate the sensitivity of the induced flow to pulse frequency and duty cycle, a test grid is devised. This involves the measurement of the induced velocity for all possible combinations of a series of D and f_p's. An overview of all parameters involved in the measurement is given in Table I.

C. High frequency interference

In this study, the first measurement point is placed at 7 mm from the actuator. In such close proximity, the hot-wire readings present a strong fluctuating component at the carrier frequency f_{ac} of the actuation signal, which in this case is 2 kHz. It is known from other investigations[26] that in the plasma formation area velocity fluctuations appear, corresponding to the carrier frequency. These are due to the physical interaction between charged and neutral particles. It is thus important to establish that the fluctuations in our signal are due to EM noise and not due to physical effects such as the plasma-flow interaction. To this goal high-speed (10 kHz) PIV data from a previous experimental campaign are used.[30] As can be seen from Fig. 3 the high frequency fluctuations appear very near the inner electrode edge (plasma formation area) but damp out and eventually disappear prior to the first hot-wire measurement point (at x=7 mm). Based on these observations the high frequency fluctuations which remain in the velocity signal will be considered as EM noise and filtered out using a low pass filter.

III. RESULTS

A. Quiescent flow

The first case in the investigation involves the pulse operation of the actuator in quiescent flow. This case, although far from any practical application, provides an overview of the true control authority of the actuator over the fluid. By ensuring a quiescent ambient flow environment, the only momentum input is provided by the actuator. Figures 4 and 5 show the time evolution of the velocity at x=7 mm and y=0.75 mm for pulse frequencies f_p=50 Hz and 200 Hz, respectively. The velocity measurement is started prior to the actuation and continues for several seconds after actuation. The initiation of each pulse is denoted in these and all subsequent figures with the vertical dashed line and their respective number. The EM noise in the velocity signal is removed with a fourth order low pass Butterworth filter with cutoff frequency of 1 kHz.

TABLE I. Test parameters for the experimental study.

Control parameter	Value
for all possible combinations of:	
Duty cycle(D)(%)	10, 25, 50, 75, 100
Modulation frequency(f_p)(Hz)	25, 50, 100, 200, 400
Voltage (V_{pp}) (kV)	10
Carrier frequency (f_{ac}) (kHz)	2

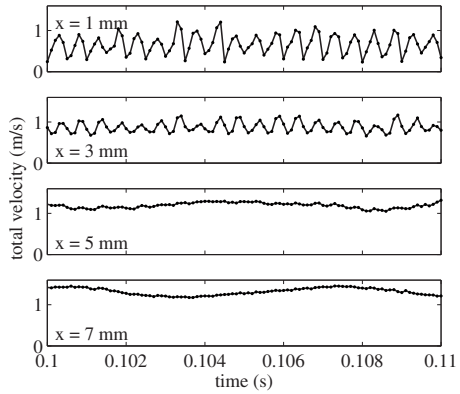

FIG. 3. Time trace of total velocity for different x positions (V_{pp}=10 kV and f_{ac}=2 kHz). High-speed PIV measurements. All data sampled at y=0.75 mm.

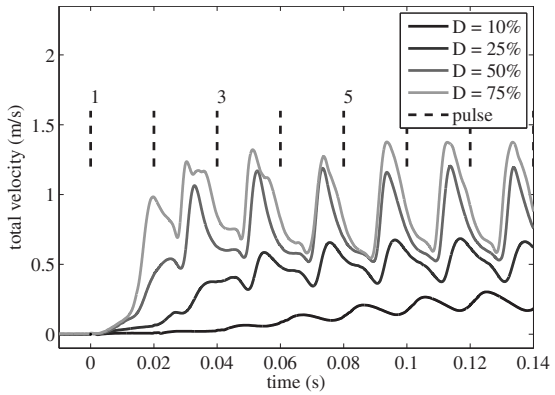

FIG. 4. Time evolution of induced velocity for pulse frequency f_p=50 Hz. Measurements at x=7 mm and y=0.75 mm.

The resulting flow accelerates from the initial still conditions to a quasisteady state where it fluctuates around a mean value, seemingly at the frequency of the actuation. It is evident that the response of the flow under the actuation is relatively fast with the quasisteady state already reached after the first few actuation cycles. The flow appears to be self limiting in its maximum velocity where a balance between the actuator produced body force and hydrodynamic forces is reached. As soon as the pulse is finished and the actuator is off the flow starts decelerating. If no other forcing is applied the flow reaches zero with typical relaxation time of 20–30 ms.

Looking at the first actuation cycles into more detail, an accumulative effect on the overall velocity is observed. This differs between cases of different duty cycles. For lower duty cycles it appears that the momentum transfer between the

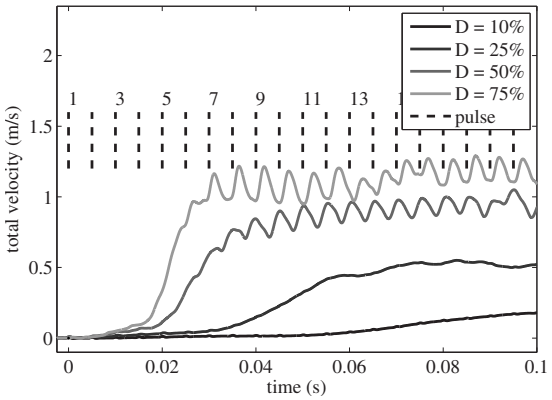

FIG. 5. Time evolution of induced velocity for pulse frequency f_p =200 Hz. Measurements taken at x=7 mm and y=0.75 mm.

ionized gas and the neutral air during one actuation cycle is not enough to bring the flow to the maximum velocity. Nevertheless, inertial forces keep the flow from decelerating to zero before the next actuation thus creating the accumulation of velocity. This apparent role of the relaxation time of the flow after each pulse seems to define the overall appearance of the fluctuating field. This also implies that for different external flow (such as a boundary layer) the fluctuations will differ since the relaxation time will also change.

Another aspect of the flow evolution is the difference between the accelerating part of the flow (the actuator is on) and the decelerating part (the actuator is off). More easily observed at low pulse frequencies (Fig. 4), the acceleration appears to be almost constant while the deceleration is of higher order. The difference can be attributed to the different mechanisms acting during the on and off periods. Acceleration is due to the body-force exerted on the fluid by the operation of the actuator while deceleration is more conventionally pressure driven. The way the flow accelerates during the actuation could be changed by employing a different waveform for the pulse, such as a sine modulation or a trapezoidal wave.

Duty cycle and pulse frequency appear to have a strong influence on the quasisteady state of the flow. As can be seen from Fig. 6 for higher duty cycles the mean flow increases and even surpasses the continuous actuation in some cases. Pulse frequency seems to have less influence on the mean velocity, as is expected since the provided power does not change with f_p. Nevertheless, differences still appear which indicate that mechanisms directly related to the flow such as

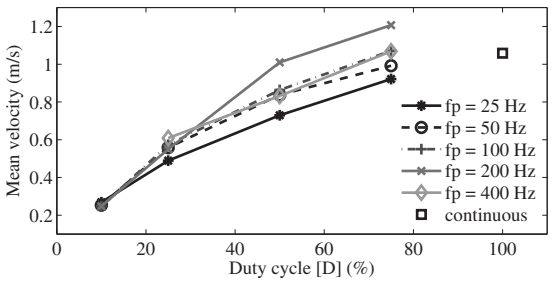

FIG. 6. Mean induced velocity at x=7 mm and y=0.75 mm (quiescent flow).

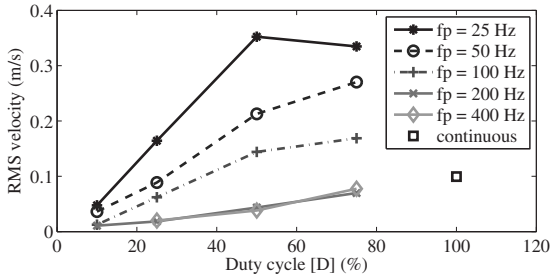

FIG. 7. rms value of induced velocity fluctuations at x=7 mm, y =0.75 mm (quiescent flow).

hydrodynamic instabilities and resonance are in action and potentially can be used for flow control. For the quiescent flow an optimum appears near f_p=200 Hz.

The rms fluctuation of the flow is also a function of pulse frequency and duty cycle as shown in Fig. 7. For higher f_p the fluctuations become weaker since the pulses become shorter in duration and repeat more often thus approaching the continuous operation. It can be noted that for continuous operation the induced velocity appears not to be laminar with considerable fluctuations present. The origin of these fluctuations is currently unknown since they do not correlate with any characteristic time scale of the actuation signal. It is interesting to note that for the cases of f_p =200 Hz and 400 Hz the fluctuations of the flow are of the same order and their trend of increase with D collapses on the continuous operation point. This inability of the actuator to produce large fluctuations on the flow for high pulse frequencies is significant especially for concepts that involve manipulation of fast developing structures such as shedding vortices or high Reynolds number unstable TS waves. Nevertheless, since the action of the actuator is directional, it is expected that the capability to introduce large fluctuations at high frequency can be larger in the case of an external flow moving in the direction of the induced jet. A test case with the actuator operating in a laminar boundary layer will be investigated to this cause. The maximum error for the calculated statistical values is 0.053% with a 99% confidence level.

The power consumption of the actuator is shown in Fig. 8. A power law seems to govern the relation between power and duty cycle giving more ground to the utilization of the actuator in pulsed operation rather than in continuous mode. For instance at f_p=200 Hz and D=75% the mean velocity is higher than the continuous actuation while power consumption is 40% less.

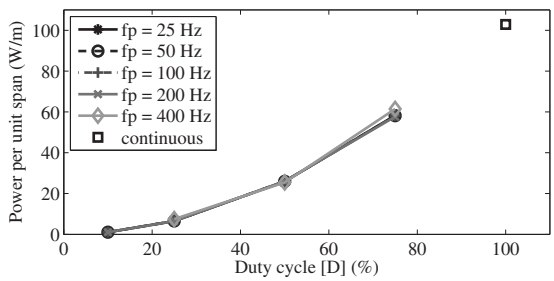

FIG. 8. Power consumption of the plasma actuator for the series of tested f_p and D.

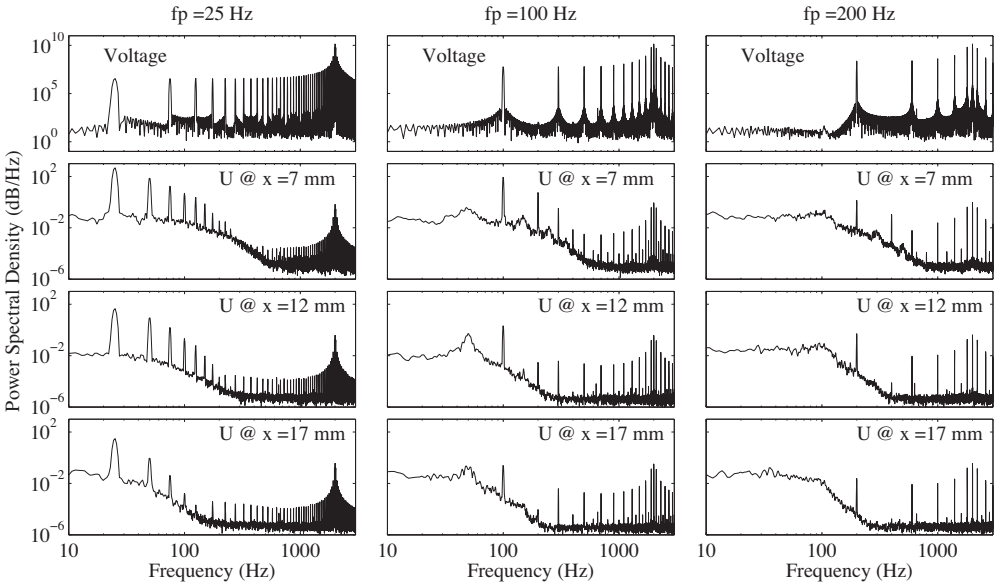

FIG. 9. Power spectral density of voltage and velocity for $D=50\%$ (quiescent flow).

Since the actuators are mainly focused on manipulating instabilities and unsteady structures of the flow a look in the spectral content of the induced flow is necessary. This will provide an insight into the correlation between the provided input signal, which in this case is the HV, with the produced velocity field. Power spectral densities of the voltage signal and the induced flow field are shown in Fig. 9 for different pulse frequencies. These are calculated using Welch's method[31] using eight segments over the entire signal with 50% overlap. The number of points taken for the fast Fourier transform (FFT) is 2^{16}. The power spectral density (PSD) is presented here for the unfiltered signals. To be noted here that the average power in the signal is the integral of the PSD over a given frequency band. The peaks in this spectra do not reflect the power at a given frequency.

The voltage signal content is inherently rich in harmonics of the pulse frequency. Of interest is the lack of the even frequency harmonics of the pulse frequency. For example, in the $f_p=100$ Hz case the harmonics of 200, 400, 600 Hz and so on are missing. This is expected as the duty cycle is fixed at 50% and will be shown to change for different duty cycles. The carrier frequency (2 kHz) is also apparent with an almost continuous subspectrum on its sides.

The velocity signal shows strong components at the main pulse frequency and its first few harmonics. A peak at the carrier frequency with a sideband subspectrum indicates the EM noise previously mentioned. At position x=7 mm the average power of the signal is calculated using a rectangle approximation of the integral of the PSD. 97.9%, 97.6%, and 76.9% of the average signal power is contained in the first three harmonics for the cases of $f_p=25$ Hz, 100 Hz, and 200 Hz respectively. The pulse harmonics decrease with distance faster than the main frequency. A secondary effect can be observed here, in the existence of even harmonics in the velocity signal that are absent in the voltage signal. These harmonics appear to decrease in power with distance, at a larger rate than the odd harmonics.

The spectral densities of the voltage and velocity signals are shown in Fig. 10 for different duty cycles. Similarly to the previous case, specific harmonics are absent from the input signal depending on the duty cycle for a fixed pulse frequency of 50 Hz. For the case of 50% all the even harmonics are absent while for the cases of 25% and 75% every fourth harmonic (f_{4n}) is absent. Similar to the pulse frequency variation, the velocity spectra correspond to the input signal. It is verified that the harmonics that have no counterpart in the input signal decay faster in the downstream distance.

Since the initial voltage signal is created using only two frequencies (f_p and f_{ac}), the fact that the flow presents a larger set of harmonics could be crucial to some flow control approaches which involve unstable structures. For instance, if the actuator is operating in a laminar boundary layer at a pulse frequency which corresponds to a stable mode, the subharmonics in the induced flowfield might be well within the unstable region and eventually cause transition.

B. Laminar boundary layer

Through the introduction of steady or unsteady disturbances in the flow the actuators can manipulate, enhance or accentuate flow instabilities, unsteady vortical structures, and other secondary flow mechanisms. As such, it is essential to identify the behavior of the actuator and the resulting flow in the case of an external and already developed flow field. As an initial test case a low velocity laminar boundary layer is selected. This choice is made based on the low energy content of such a flow which would in turn increase the experimental observability of any effect the actuator might have. A typical scenario for such base flow would be the active cancellation of TS waves. Since the convecting instabilities which in the case of unswept wings are TS waves have the form of a multi frequency wave train, the actuator is required to operate in pulse or burst mode.[23]

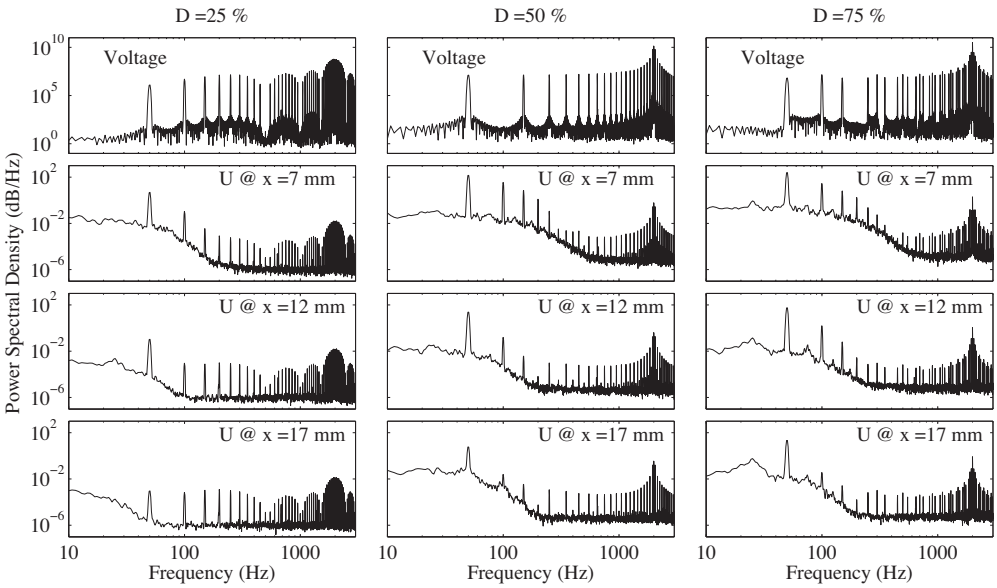

FIG. 10. Power spectral density of voltage and velocity for f_p=50 Hz (quiescent flow).

The BLT is used to create a laminar boundary layer in which the actuator is operating in pulse mode. The freestream velocity is intentionally kept low at 4.6 m/s in order to avoid boundary layer instabilities to grow to levels that would interfere with the induced velocity components of the actuator. The boundary layer velocity profile is presented in Fig. 11. The boundary layer is naturally growing downstream although for the first three x positions the growth is minimal.

For the pulse operation the same combination of duty cycles and pulse frequencies as with the quiescent flow is tested. Two additional x positions are measured at 47 and 97 mm downstream the actuator. All measurements are taken at 0.75 mm from the wall which approximately corresponds to $0.25\delta^*$ of the boundary layer at x=7 mm.

Prior to the pulse operation a test case of continuous actuation is performed in order to establish a reference flowfield. This is shown in Fig. 12. It is apparent that the flow accelerates downstream the actuator but does not remain laminar. Strong fluctuations exist especially in the vicinity of the actuator. These damp downstream but remain considerably larger than the fluctuations of the unperturbed flow. The frequency content of these fluctuation seems not to be related with the actuation specific carrier frequency.

The velocity measurements for pulse frequencies of 25 and 200 Hz and different duty cycles are presented in Figs. 13 and 14, respectively. A similar to the quiescent flow case behavior can be observed. In the vicinity of the actuator velocity consists of a mean component which is considerably larger than the unperturbed boundary layer velocity and strong fluctuating components. The velocity fluctuations correspond to the actuator pulses and appear at the specific pulse frequency. The mean velocity and rms value of the fluctuations are shown in Figs. 15 and 16 respectively. Of interest is the insensitivity of the mean flow to changes in pulse frequency. This differs from the respective case in quiescent flow and can be attributed to the shorter relaxation time of the flow. This suggests that the mean velocity increase from the operation of the actuator is purely a function of the energy input the later is capable, for this specific test case. In contrast, the intensity of fluctuations seems to depend on both the pulse frequency and the duty cycle. Again the relatively short relaxation time of the flow appears to govern this behavior where long and low frequency pulses give the largest fluctuations while short and high frequency pulses appear to collapse on the continuous actuation point. The maximum error for the calculated statistical values here is 0.037% with a 99% confidence level. To be noted here that for the investigated cases, the power consumption of the actuator is found to be independent of the external flow.

The intensity of the velocity fluctuations appears to be dependent on the duty cycle with the same energy accumulation mechanism as in the quiescent flow seemingly govern-

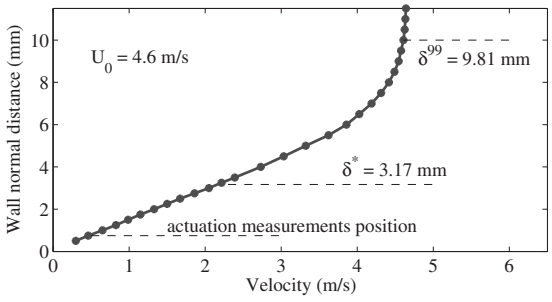

FIG. 11. The laminar boundary layer at position x=7 mm.

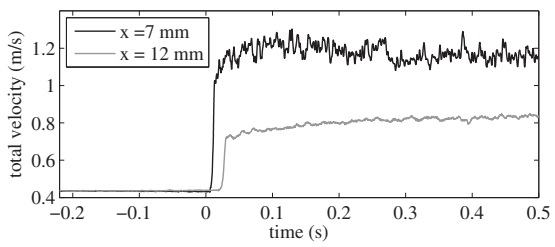

FIG. 12. Velocity evolution for continuous operation at two downstream positions.

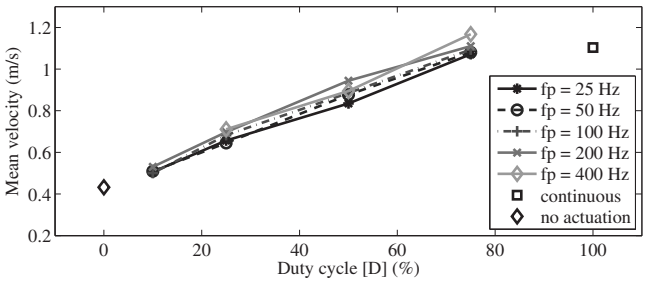

FIG. 13. Time evolution of velocity for pulse frequency f_p=25 Hz. Measurements at x=7 mm, y=0.75 mm.

ing the operation. More specifically the full development of the field to its quasisteady state is achieved after some actuation cycles especially for low duty cycles and high pulse frequency. Nevertheless, comparing with the respective case in quiescent flow, as shown in Fig. 5, maximum velocity is achieved in a much shorter time from the start of the actuation. An effect that can additionally be observed is the fact that larger fluctuations appear for higher pulse frequencies than in quiescent flow. For instance at f_p=200 Hz and D =25% the induced velocity in quiescent flow almost lacks any coherent fluctuating component and rather resembles the flowfield from continuous operation. For the boundary layer case, as can be observed from Fig. 14, the flow still exhibits fluctuations corresponding to the pulse frequency at D =25%. This can be explained taking account that the velocity of the external flow with no actuation is larger than the case of quiescent flow (zero velocity). This in turn makes the relaxation time of the flow less. One more contributing effect in the enhancement of the fluctuations is the arrangement of the actuator in a coflow configuration. The actuator introduces the fluctuations by adding momentum to the flow since the induced velocity is in the same direction as the external flow.

In several flow control scenarios the operation of more than one actuators is proposed in order to extent their control authority in streamwise distance. It is thus useful to track the downstream development of the induced fluctuations from the operation of the actuator. In this manner the effective downstream region for a single actuator can be defined. A track of the evolution of the fluctuating field can be seen in Fig. 17 for pulse frequency of 50 Hz and duty cycle of 50%. Similar behavior is observed for the rest of the tested pulse frequencies. The effect of the actuator is local as strong fluctuations appear only at the first three measurement positions

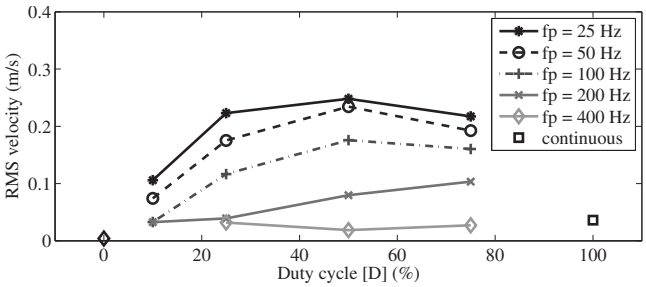

FIG. 14. Time evolution of velocity for pulse frequency f_p=200 Hz. Measurements at x=7 mm, y=0.75 mm.

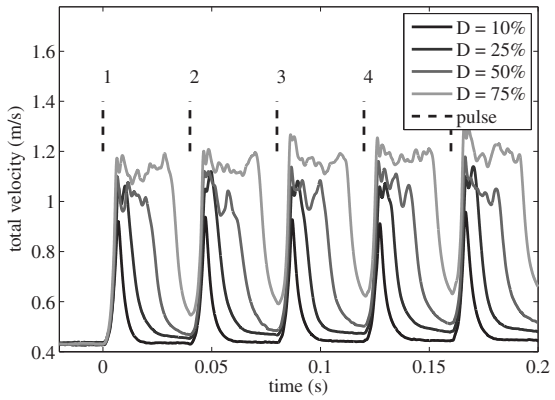

FIG. 15. Mean induced velocity at x=7 mm and y=0.75 mm (boundary layer).

or within 10 mm from the actuator. Further downstream, at 47 mm, the mean velocity acceleration is evident but the fluctuating components have almost disappeared. At 97 mm only a very weak increase in velocity is registered. In the case of the laminar boundary layer the distance in which the forcing of the actuator can be perceived is highly dependent on the freestream conditions and the hydrodynamic stability of the flow. In this case, it is obvious that 50 *Hz* corresponds to a stable mode at this Reynolds number. This can also be verified by linear stability theory. Nevertheless it seems that independent of forcing frequency the actuator can introduce strong fluctuations at least in the first 10 mm downstream.

As already mentioned, many flow control applications rely on the manipulation of inherent instabilities of the flow to efficiently achieve the desired control. In this aspect it is highly desirable to be able to control any potential actuator in an accurate manner, introducing forcing components that are necessary and avoiding any unwanted artifacts that might be additionally introduced. Based on this, some comments can be made on the pulse operation of the actuator. It is clear from the continuous operation of the actuator Fig. 12 that the induced flowfield is unsteady with the velocity signal being almost stochastic in time. This behavior can also be observed in pulse operation for low pulse frequencies and high duty cycles. For instance at f_p=25 Hz and D=75% (Fig. 13) the flow accelerates after each pulse begins until it reaches its self limiting maximum velocity. This is reached before the

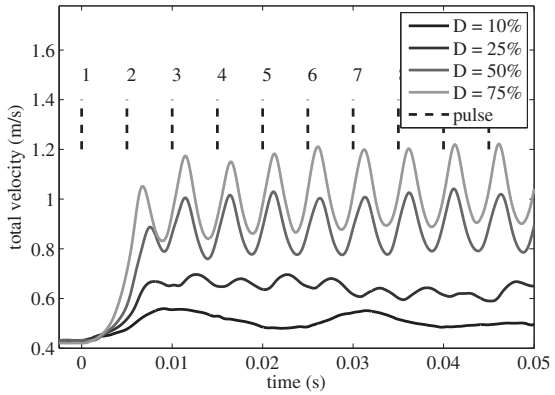

FIG. 16. rms value of velocity fluctuations at x=7 mm and y=0.75 mm (boundary layer).

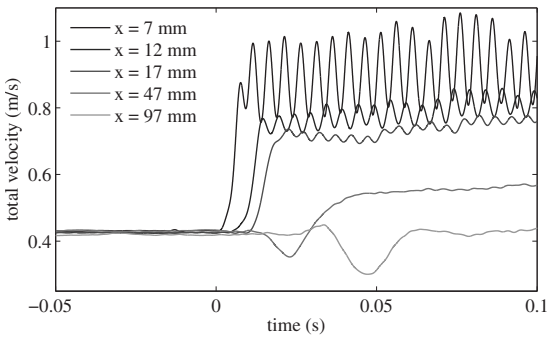

FIG. 17. Time evolution of velocity for pulse frequency $f_p=50$ Hz, $D=50\%$, and different downstream positions (measurement at y=0.75 mm).

end of the pulse and for the remaining duration of the pulse the flow essentially behaves as in the continuous operation. This could potentially be unwanted since the stochastic velocity signal might trigger instabilities in the flow in a random and uncontrolled fashion. It is thus important to limit the duration of the pulse to the point where a "clean" forcing is imposed on the flow. Furthermore, reduction in the duty cycle could contribute positively in the reduction in power.

One additional feature which is important in efficient flow control is the actual intensity of the fluctuating components. Especially for high pulse frequencies and low duty cycles such as the case of $f_p=200$ Hz and $D=10\%$ (Fig. 14) the momentum input from the actuator is too little and the relaxation of the flow is too slow to respond to the actuation. This results in a flowfield which resembles the continuous operation case albeit with a lower mean velocity since the input energy is limited. For these cases the ability of the actuator to impose unsteady forcing on the flow is severely limited.

Based on the previous two phenomenological observations an empirical model for the operating envelope of the actuator can be formulated (Fig. 18). This is far from strict values and rather a 'rule of thumb' for the useful range of the actuator operating pulse frequency and duty cycle. To be noted that these values apply only for the applied voltage (10 kV) and carrier frequency (2 kHz) of this test case and have to be redefined if these parameters are to be varied.

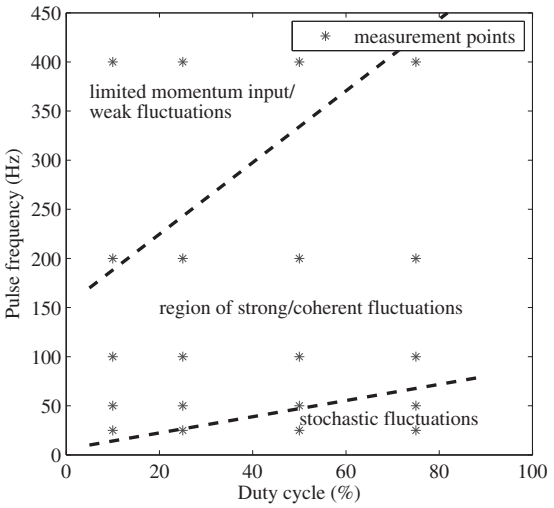

FIG. 18. Empirical operational envelope for the plasma actuator operation in a low speed laminar boundary layer.

IV. CONCLUSIONS

An experimental study has been conducted on the operation of the plasma actuator in pulse mode. The actuator used was a conventional DBD incorporating copper electrodes and Kapton dielectric. The high voltage and carrier frequency were kept fixed at $V_{pp}=10$ kV and $f_{ac}=2$ kHz respectively. Total velocity was measured for the cases of quiescent flow and laminar boundary layer. Several combinations of pulse frequency and duty cycles were tested in order to evaluate the sensitivity and form of the resulting flowfield.

From the tests it became apparent that the plasma actuator is capable in introducing mean and fluctuating components of velocity to the surrounding air when operated in pulse mode. In most cases a quasisteady situation is reached after a few cycles of actuation. For the quiescent flow a strong dependence connecting pulse frequency and duty cycle with mean velocity and fluctuation intensity has been found. An upper limit in pulse frequency and a lower limit in duty cycle seem to define the useful operating range of the actuator. The respective tests in the laminar boundary layer reveal the importance of the outer flow and especially the relaxation time in the final form of the fluctuating field. Differences between the two cases suggest that results from tests in quiescent flow might not be suitable for correct prediction of the actuator performance in other flows.

An additional spectral analysis has been performed on the velocity signal from the test in quiescent flow. As shown the induced velocity field presents a slightly different spectral content than the forcing signal. This is important in applications dealing with hydrodynamic stability where the exact spectral content of the forcing must be precisely controlled.

For the laminar boundary layer cases the measured velocities present distinct differences from the respective quiescent flow cases. Due to the existing energy content of the boundary layer as well as the directional forcing of the actuator the control authority over the flow is increased. This is especially important when high frequency actuation is required. Nevertheless, due to the same reasons some unwanted effects are also identified. For large duty cycles and low pulse frequencies a similar to the continuous actuation field is measured for part of the actuation pulse. This consists of random and uncorellated velocity fluctuations which potentially could degrade the performance of the actuator. One more important aspect is the lower limit in duty cycle which was previously identified in the quiescent case. Depending on the pulse frequency the actuators seems to lack the necessary power to induced strong and coherent fluctuations when operating below a certain value of duty cycle. This is particularly pronounced in high pulse frequencies. Based on these observations an empirical operational envelope is proposed for the implementation of the actuator in pulse mode flow control techniques. The envelope is specific to the operating parameters and external flow for the test case under

investigation but similar approach in deriving "situation specific" envelopes could be followed for any other case.

ACKNOWLEDGMENTS

This work is conducted in the framework of the CleanEra project initiated by TU Delft (www.cleanera.tudelft.nl). The authors would like to acknowledge dr.ir. Peter H. F. Morshuis from the High Voltage Laboratory of the Faculty of Electrical Engineering, Mathematics and Computer Science for his valuable contributions and Stefan Bernardy and Leo Molenwijk for their technical assistance.

[1]T. C. Corke, M. L. Post, and D. M. Orlov, Exp. Fluids **46**, 1 (2009).
[2]E. Moreau, J. Phys. D: Appl. Phys. **40**, 605 (2007).
[3]J. D. Jacob, R. Rivir, C. Carter, and J. Estevadeordal, 2nd AIAA Flow Control Conference, Portland, Oregon, 28 June – 1 July 2004.
[4]Y. Li, X. Zhang, and X. Huang, Exp. Fluids **2**, 1 (2010).
[5]B. Göksel, D. Greenblatt, I. Rechenberg, Y. Kastantin, C. N. Nayeri, and C. O. Paschereit, Notes on Numerical Fluid Mechanics **95**, 42 (2007).
[6]M. L. Post and T. C. Corke, AIAA J. **42**, 2177 (2004).
[7]J. H. Mabe, F. T. Calkins, B. Wesley, R. Woszidlo, L. Taubert, and I. Wygnanski, 37th AIAA Fluid Dynamics Conference and Exhibit, Miami, Florida, 25–28 June 2007.
[8]C. O. Porter, T. E. McLaughlin, C. L. Enloe, G. I. Font, J. Roney, and J. W. Baughn, 45th AIAA Aerospace Sciences Meeting and Exhibit, Reno, Nevada, 8–11 January 2007.
[9]A. Seraudie, E. Aubert, N. Naude, and J. P. Cambronne, Third AIAA Flow Control Conference, San Francisco, California, 5–8 January 2006.
[10]T. N. Jukes, K. Choi, G. A. Johnson, and S. J. Scott, Third AIAA Flow Control Conference, San Francisco, California, 5–8 January 2006.
[11]T. Abe, Y. Takizawa, S. Sato, and N. Kimura, AIAA J. **46**, 2248 (2008).
[12]B. Dong, J. M. Bauchire, J. M. Pouvesle, P. Magnier, and D. Hong, J. Phys. D: Appl. Phys. **41**, 155201 (2008).
[13]M. Forte, J. Jolibois, J. Pons, E. Moreau, G. Touchard, and M. Cazalens, Exp. Fluids **43**, 917 (2007).
[14]F. O. Thomas, T. C. Corke, M. Iqbal, A. Kozlov, and D. Schatzman, AIAA J. **47**, 2169 (2009).
[15]C. L. Enloe, M. G. McHarg, and T. E. McLaughlin, J. Appl. Phys. **103**, 073302 (2008).
[16]A. R. Hoskinson, N. Hershkowitz, and D. E. Ashpis, J. Phys. D: Appl. Phys. **41**, 245209 (2008).
[17]D. F. Opaits, A. V. Likhanskii, G. Neretti, S. Zaidi, M. N. Shneider, R. B. Miles, and S. O. MacHeret, J. Appl. Phys. **104**, 043304 (2008).
[18]J. Little, M. Nishihara, I. Adamovich, and M. Samimy, Exp. Fluids **48**, 521 (2010).
[19]E. Moreau, R. Sosa, and G. Artana, J. Phys. D: Appl. Phys. **41**, 115204 (2008).
[20]H. Schlichting and K. Gersten, *Boundary Layer Theory* (Springer, Berlin, 2000).
[21]D. Sturzebecher and W. Nitsche, Int. J. Heat Fluid Flow **24**, 572 (2003).
[22]S. Grundmann and C. Tropea, Exp. Fluids **44**, 795 (2008).
[23]S. Grundmann and C. Tropea, Int. J. Heat Fluid Flow **30**, 394 (2009).
[24]T. N. Jukes and K. Choi, Phys. Fluids **21**, 084103 (2009).
[25]M. L. Post and T. C. Corke, AIAA J. **44**, 3125 (2006).
[26]N. Benard and E. Moreau, J. Phys. D: Appl. Phys. **43**, 145201 (2010).
[27]N. Balcon, N. Benard, and E. Moreau, IEEE Trans. Dielectr. Electr. Insul. **16**, 463 (2009).
[28]V. Boucinha, P. Magnier, R. Weber, A. Leroy-Chesneau, B. Dong, and D. Hong, Fourth Flow Control Conference, Seattle, Washington, 23–26 June 2008.
[29]T. N. Jukes, K. Choi, T. Segawa, and H. Yoshida, Proceedings of the Institution of Mechanical Engineers, Part I: Journal of Systems and Control Engineering **222**, 347 (2008).
[30]M. Kotsonis, S. Ghaemi, R. Giepman, and L. Veldhuis, 41st AIAA Plasmadynamics and Laser Conference, Chicago, Illinois, 28 June – 1 July 2010.
[31]P. D. Welch, IEEE Trans. Audio Electroacoust. **15**, 70 (1967).